A Level Set Technique for 3D Magnetic Induction Tomography at Different Scales

Oliver Dorn

The University of Manchester, United Kingdom

ICERM workshop on Mathematical and Computational Aspects of Radar Imaging, Providence

18 October 2017

MANCHESTER 1824
The University of Manchester

Applications of Interest

- Electromagnetic imaging in the near field has a variety of applications.
- We are interested in using time-harmonic EM fields for the 3D imaging of domains or objects.
- Of particular concern to us is penetration depth. The objects we are interested in might be enclosed in metallic boxes or in a conductive environment.
- Practical applications include:
  - Geophysics/Environmental - Locating objects in the earth ($> 200m^3$)
  - Cargo Containers ($\sim 10m^3$)
  - Boxes/Suitcases/Luggage ($\sim 1m^3$)
  - Small boxes ($\sim 0.5m^3$)

Proof of Concept - Geophysical Scale ($> 200m^3$)

Source: https://en.wikipedia.org/wiki/Lost_Hills_Oil_Field

Proof of Concept - Cargo Container Scale ($20m^3$)

Source: Wikipedia https://en.wikipedia.org/wiki/Cargo_scanning

Proof of Concept - Luggage and Box Scale ($2m^3$)

Source: https://en.wikipedia.org/wiki/Airport_security

Maxwell's Equations

$$
\begin{aligned}
\nabla \times E - i\omega\mu H &= M^s \\
\nabla \times H - \hat{\sigma}(x) E &= J^s
\end{aligned}
$$

$$
\hat{\sigma} = \sigma - i\omega\epsilon
$$

- Use one frequency (for the moment).
- We want to use 'low frequencies' in order to increase penetration depth. Fields tend to behave diffusive. Inverse problem becomes severely ill-posed.
- Singularities inside the domain are not represented by 'measurable' singularities in the data.

Mathematical Forward Problem

- For the moment we restrict ourselves to imaging σ.
- We write Maxwell's equations in operator form as

$$\Lambda(\sigma)\, u \;=\; q$$

with $u = (E, H)$ and q being the source (e.g. coil)

- Forward operator A mapping the parameter σ to the corresponding data $g = Mu$:

$$\mathcal{A}(\sigma) \;=\; M\, u \;=\; M\,\Lambda(\sigma)^{-1} q$$

where M is the linear measurement operator (e.g. coils)

Optimization problem formulation of inverse problem

- Physically measured 'true data' (for $\tilde{u}$ being true field)

$$\tilde{g} = M\tilde{u}$$

- Residual operator $\mathcal{R}$:

$$\mathcal{R}(\sigma) = \mathcal{A}(\sigma) - \tilde{g}.$$

- Optimization problem (regularized output least squares)

$$\text{Min}_{\sigma} \quad \mathcal{J}(\sigma) = \frac{1}{2}\|\mathcal{R}(\sigma)\|_2^2 + \frac{\eta}{2}\|\sigma\|_\alpha$$

where $\|\sigma\|_\alpha$ denotes some norm or semi-norm of σ and η is some regularization parameter.

The shape-based inverse problem

- Often we are interested in detecting and characterizing specific objects (targets) of unknown shapes (a priori assumption).
- Can we determine and characterize shape-like targets (with sharp interfaces to the background) from data that do not contain visible singularities?
- In more details, assume that the parameter σ has the following specific form

$$\sigma(x) = \begin{cases} \sigma_i & \text{in} \quad S \\ \sigma_e(x) & \text{in} \quad \Omega \backslash S \end{cases}$$

  where S is the shape of interest.

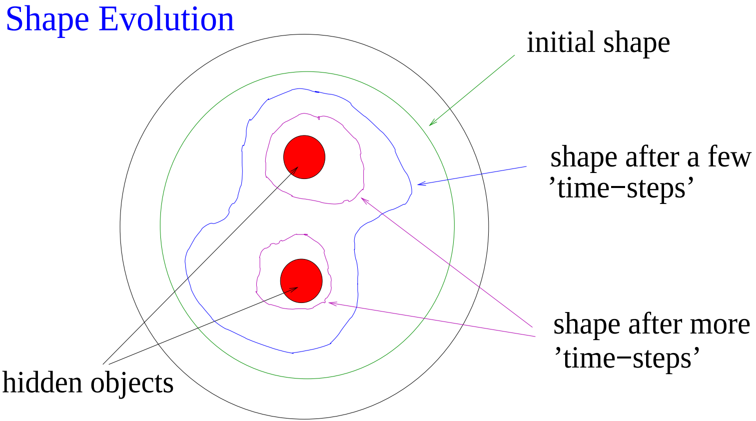
Shape Evolution
initial shape
shape after a few
'time−steps'
shape after more
'time−steps'
hidden objects

Shape evolution by artificial shape velocity field

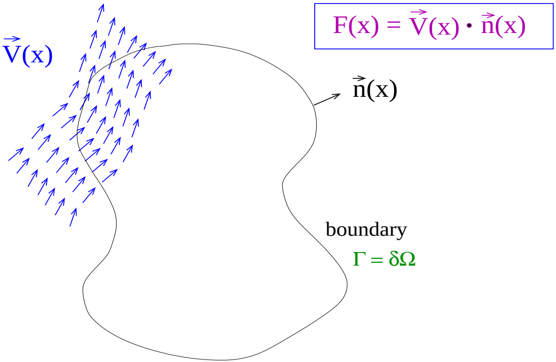

Moving the boundary with velocity field $\vec{V}(x)$

Practical shape optimization

There are two basic problems to solve in the shape evolution approach:

1. Constructing an appropriate velocity function from boundary data.
2. Moving the shape computationally according to the velocity function

Notice that: During the evolution, the ease of handling topological changes is crucial since we do not know the topology of the shapes a-priori.

Introduce a sufficiently smooth level set function ψ such that

$$\sigma(x) = \begin{cases} \sigma_i, & \text{if} \quad \psi(x) \le 0 \\ \sigma_e, & \text{if} \quad \psi(x) > 0 \end{cases}$$

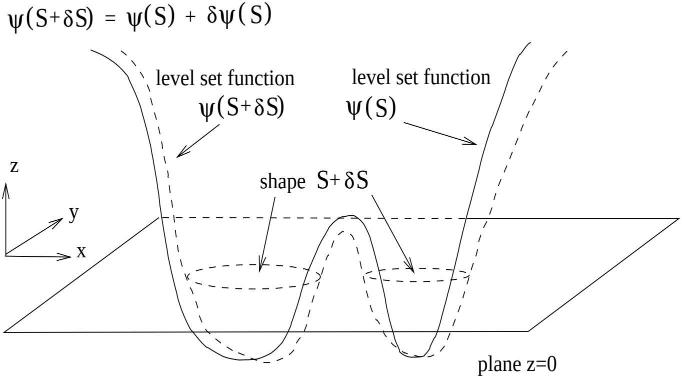

Formal setup

- The boundary $\Gamma(t)$ of the shape S at time t is

$$\Gamma(t) = \{x \ : \ \psi(x,t) = 0\}$$

- The residual operator $\mathcal{R}$

$$\mathcal{R}(\psi) = \mathcal{R}(\sigma(\psi)) \ = \ \mathcal{A}(\sigma(\psi)) - \tilde{g}$$

  is now understood as a function in ψ.

- The least squares cost functional (without explicit regularization term) is given by

$$\mathcal{J}(\psi) \ = \ \frac{1}{2}\|\mathcal{R}(\psi)\|^2$$

Some formal calculations

- We consider the general evolution law

$$\frac{d\psi}{dt} = f(x, t, \psi, \mathcal{A}, \tilde{g}, \ldots)$$

- We introduce the one-dimensional Heaviside function $h(\psi)$

$$h(\psi) = \begin{cases} 1 & , \quad \psi > 0 \\ 0 & , \quad \psi \leq 0 \end{cases}$$

- Then, we can write

$$\sigma(\psi) = \sigma_e h(\psi) + \sigma_i (1 - h(\psi)).$$

- Formal differentiation yields

$$\frac{d\sigma}{d\psi} = (\sigma_e - \sigma_i)\delta(\psi)$$

More formal calculations

- Formal differentiation of the least squares cost functional $\mathcal{J}(\sigma(\psi(t)))$ yields

$$\frac{d\mathcal{J}}{dt} = \frac{d\mathcal{J}}{d\sigma}\,\frac{d\sigma}{d\psi}\,\frac{d\psi}{dt} = \left\langle \mathcal{R}'(\sigma)^*\mathcal{R}(\sigma)\,,\,\frac{d\sigma}{d\psi}\,\frac{d\psi}{dt}\right\rangle_P$$

by the chain rule.

- Here, $\mathcal{R}'(\sigma)$ is the linearized residual operator, and $\mathcal{R}'(\sigma)^*$ is its adjoint.
- *Remark:* The sensitivities $\mathcal{R}'(\sigma)^*\mathcal{R}(\sigma)$ can be calculated efficiently by just solving one forward and one adjoint Maxwell problem ('adjoint scheme').

Adjoint scheme for calculating sensitivities

- The operator $\mathcal{R}'(\sigma)^*$ is defined by

$$\langle \mathcal{R}'(\sigma)\delta\sigma, \rho \rangle_Z = \langle \delta\sigma, \mathcal{R}'(\sigma)^* \rho \rangle_P \,. \tag{1}$$

- We have

$$\mathcal{R}'(\sigma)_j^* \mathcal{R}_j(\sigma) \;=\; \overline{E_j(x)} \cdot \mathcal{E}_j(x) \tag{2}$$

where $\mathcal{E}_j$ and $\mathcal{H}_j$ are the solution of the 'adjoint Maxwell system'

$$\begin{pmatrix} -\overline{b} & \nabla\times \\ \nabla\times & \overline{a_0} \end{pmatrix} \begin{pmatrix} \mathcal{E}_j \\ \mathcal{H}_j \end{pmatrix} = M_j^* \mathcal{R}_j(\sigma)$$

Even more formal calculations

- Collecting terms yields

$$\frac{d\mathcal{J}}{dt} = \Big\langle \mathcal{R}'(\sigma)^*\mathcal{R}(\sigma)\,,\,(\sigma_e - \sigma_i)\delta(\psi)\,f(x,\ldots)\Big\rangle_P .$$

- Let us define now the descent direction f_d by

$$f_d(x,t,\psi,\mathcal{R},\ldots) = -F\,\chi_{NB,\partial S}$$

with the narrowband function $\chi_{NB,\partial S}(x)$ and

$$F(x) = (\sigma_e - \sigma_i)\mathcal{R}'(\sigma)^*\mathcal{R}(\sigma).$$

- This provides us with a descent flow for $\mathcal{J}$.

Regularization

- Regularization: Use regularized forcing term

$$f_r \;=\; (\alpha I - \beta\Delta)^{-1}\, f_d$$

with regularization parameters $\alpha > 0$ and $\beta > 0$.

- Discretization: We calculate discrete time-steps with step-size $\tau > 0$

$$\frac{\psi(t+\tau) - \psi(t)}{\tau} \;=\; (\alpha I - \beta\Delta)^{-1}\, f_d(t)$$

- With $\psi^{(n+1)} = \psi(t+\tau)$ and $\psi^{(n)} = \psi(t)$, this yields

$$\psi^{(n+1)} \;=\; \psi^{(n)} \;+\; \tau^{(n)}\delta\psi^{(n)}, \quad \psi^{(0)} = \psi_0$$

with

$$\delta\psi^{(n)} \;=\; (\alpha I - \beta\Delta)^{-1}\, f_d^{(n)}$$

A nonlinear Kaczmarz style approach with line search

- The step size $\tau^{(n)}$ needs to be determined by a line search procedure.
- Regardless which forward solver we use, 3D Maxwell simulation in heterogeneous media is computationally expensive.
- Full gradient calculation requires one forward and one adjoint solve *times the number of sources*. A traditional line search requires *another one or two forward solves per source*. This is too expensive!
- Instead, we apply updates immediately after an individual source position is considered ('nonlinear Kaczmarz').
- As line search we control the 'shape speed' instead of reduction in cost which can be done 'on the fly' without extra computational cost (no additional forward or adjoint problem).

Numerical forward solver

We are currently experimenting with two different numerical forward solvers.

1. A finite volume frequency domain discretization in 3D.
2. A finite difference frequency domain discretization in 3D.

Alternative forward solvers are possible, such as finite elements or variants of iterated Born/Neumann series.

Forward Problem

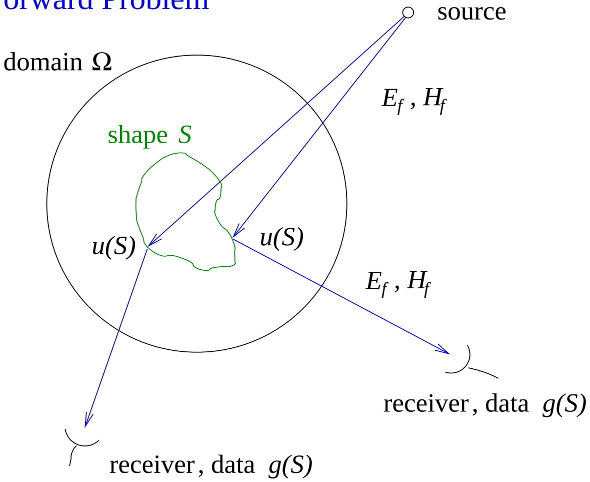

Schematic pseudo code II

Adjoint Problem

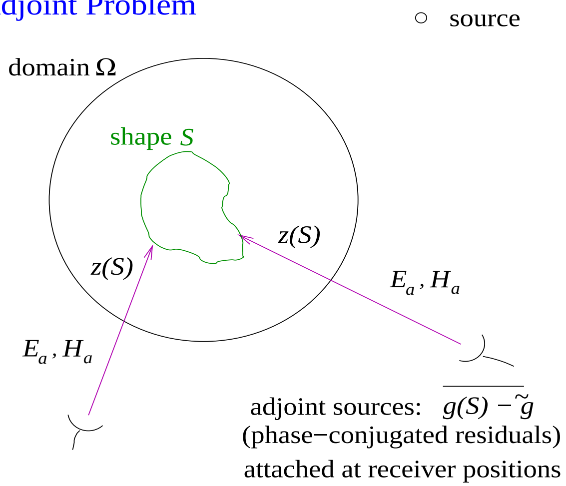

Schematic pseudo code III

Adjoint Scheme

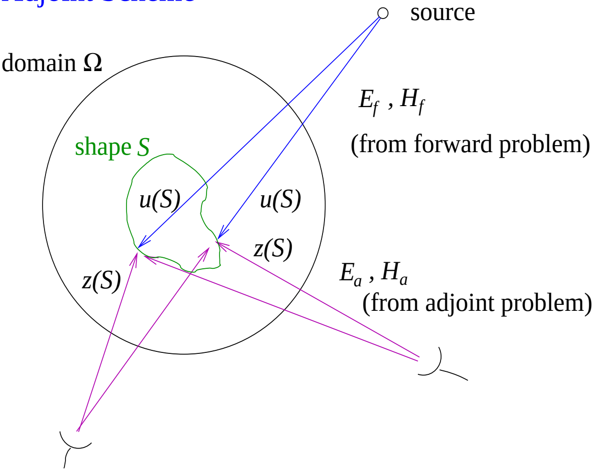

Schematic pseudo code IV

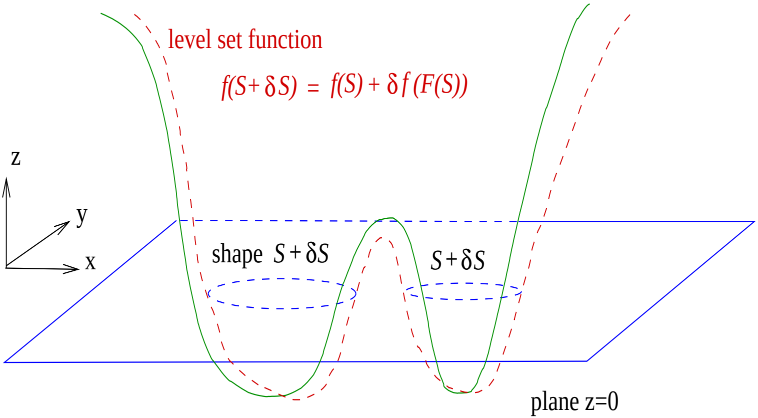

Schematic pseudo code V

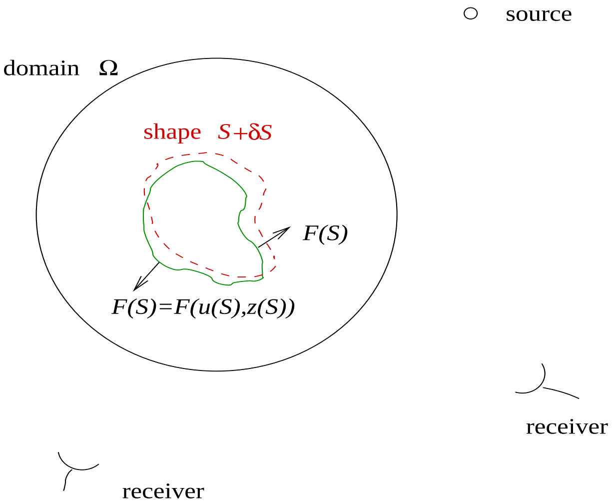

Geometry of Problem (Geophysics and Environmental)

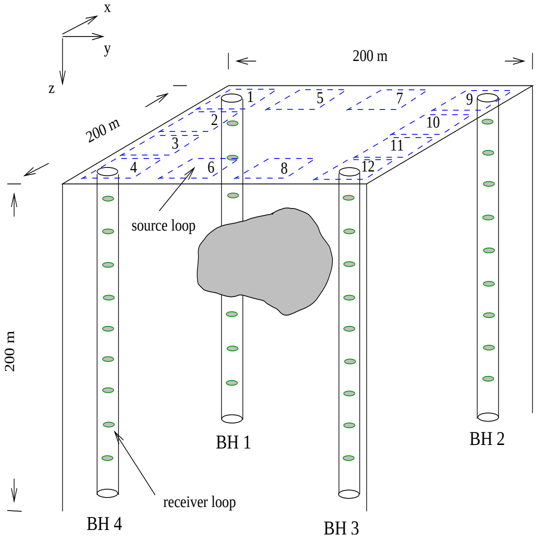

Figure: $f = 1$kHz.

Proof of concept - Geophysics scale

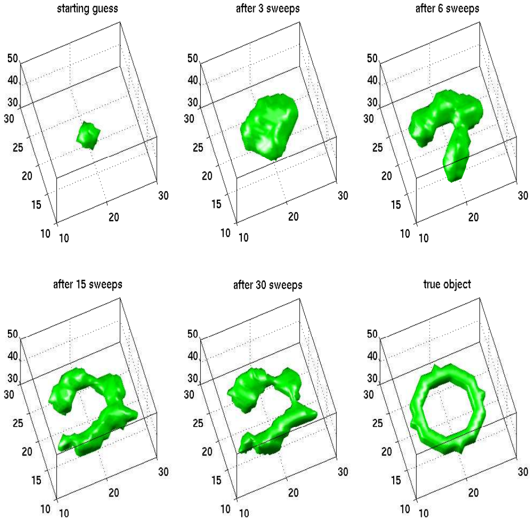

Figure: $f = 1\text{kHz}$.

Geometry of Problem (boxes and containers)

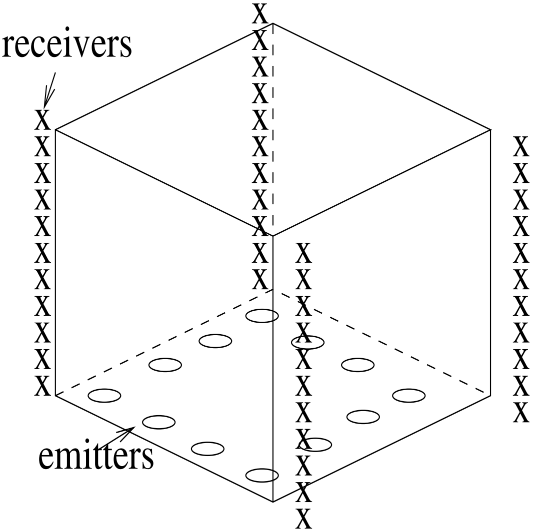

Figure: $f = 0.2$ MHz (containers) or $f = 10$MHz (boxes)

Sensitivity Functions

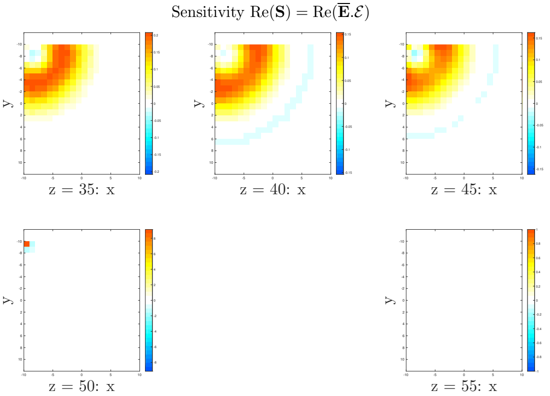

Proof of Concept - Cargo Container Scale ($20m^3$)

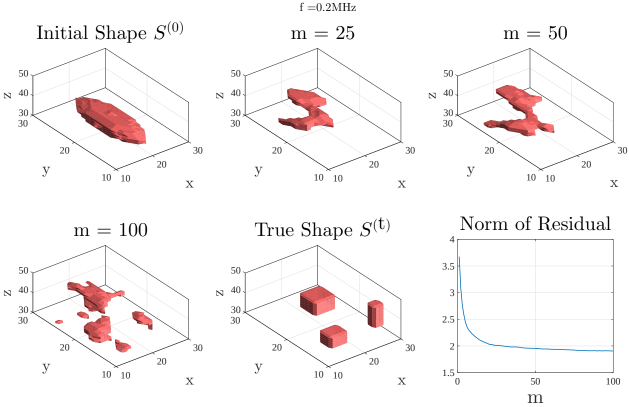

Imaging cargo container ($f = 0.2$ MHz)

Proof of Concept - Box Scale ($1m^3$)

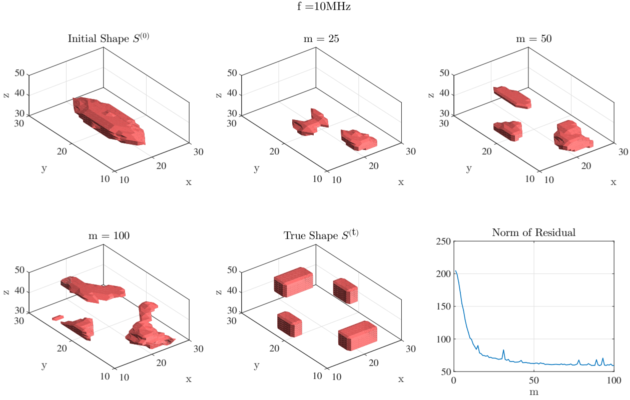

Imaging boxes ($f = 10$ MHz)

Summary

- Shapes and objects can be estimated and characterized from low frequency EM data when going beyond the Born approximation;
- This allows for penetrating shielding structures such as walls, foliage, metallic cases, or the surface of the Earth (GPR);
- Computational cost is increased due to the need for forward models incorporating inhomogeneous backgrounds;
- Multistatic antenna setups are preferred in order to obtain 3D reconstructions;
- Novel measurement technologies inspire new applications;
- This can be applied at various scales;
- Much research still needs to be done ...

References

[1] Champagne, N.J., Berryman, J.G. and Buettner, H.M., 2001. FDFD: A 3D finite-difference frequency-domain code for electromagnetic induction tomography. Journal of Computational Physics, 170(2), pp.830-848.

[2] Dorn, O. and Ascher, U., 2007. Shape reconstruction in 3D electromagnetic induction tomography using a level set technique. Proc. 23rd International Review of Progress in Applied Computational Electromagnetics ACES, pp.1-6.

[3] Dorn, O., Bertete-Aguirre, H., Berryman, J.G. and Papanicolaou, G.C., 1999. A nonlinear inversion method for 3D electromagnetic imaging using adjoint fields. Inverse Problems, 15(6), p.1523.

[4] Dorn, O. and Lesselier, D., 2006. Level set methods for inverse scattering. Inverse Problems, 22(4), p.R67.

[5] Dorn, O. and Hiles, A., 2018. A level set method for magnetic induction tomography of 3D boxes and containers. *Submitted to* Electromagnetic Nondestructive Evaluation, Vol XXI, series Studies in Applied Electromagnetics and Mechanics, IOS Press.

[6] Haber, E., Ascher, U.M., Aruliah, D.A. and Oldenburg, D.W., 2000. Fast simulation of 3D electromagnetic problems using potentials. Journal of Computational Physics, 163(1), pp.150-171.

[7] S. Hussain, L. Marmugi, C. Deans, F. Renzoni, "Electromagnetic imaging with atomic magnetometers: a novel approach to security and surveillance", *SPIE Proc. Vol 9823: Detection and Sensing of Mines, Explosive Objects, and Obscured Targets XXI*, May 2016.

[8] Darrer, B.J., Watson, J.C., Bartlett, P. and Renzoni, F., 2015. Toward an automated setup for magnetic induction tomography. IEEE Transactions on Magnetics, 51(1), pp.1-4.

[9] Wood J., Ward R., Lloyd C., Tatum P., Shenton-Taylor C., Taylor S., Bagley G., Joseph M. and Watson J.C., 2017. Effect of Shielding Conductivity on Magnetic Induction Tomographic Security Imagery, IEEE Trans. Magn. **53** (4).

QUESTIONS?